Project Module: Establishing Assay for Gene expression Quantification Using RNA *in situ* Hybridization on Mice Liver Slices

I. Introduction

Chronic liver diseases burden an approximate of 1.5 billion people worldwide. They can vary between viral hepatitis, alcoholic liver disease and non-alcoholic fatty liver disease (NAFLD) and the more severe, non-alcoholic steatohepatitis (NASH) (Moon et al., 2020). People with underlying liver disease might not be symptomatic until the disease has reached a 'point of no return'. Early diagnosis is key to make use of the liver's regeneration capacity and avoid further deterioration. Nevertheless, in 2020 hepatocellular carcinoma (HCC) was listed the third most common source of cancer-related death after lung and colorectal cancer (Sung et al., 2021). Although these diseases have different etiologies, they still share stages of organ damage progression, and in many cases they can all lead secondarily to HCC. To study the molecular mechanisms behind liver damage, we can focus on the liver cell-type population that takes up the largest part of the organ's volume and performs most of its metabolic functions, the liver parenchymal cells, hepatocytes. Hepatocytes are also the primary epithelial cell-type of the liver and are supplied with blood rich in nutrients, toxins, and microbiome metabolites, constantly being exposed to damage.
One way we can explore the differences between damaged and healthy tissue is by looking at variations between their transcriptomes (Berasain et al., 2023). With the recent advance of single cell technologies allow us to look at these differences in finer resolution. These variations can include information not only on what constitutes a specific cell type but also how a change in transcriptional activity may contribute or signalize disease. The Hepatocyte Damage Score (HDS) surged with the goal to explore this question. It is a score that should be able to call the level of damage a single hepatocyte given that one cell's expression profile of a small subset of genes.

The HDS is being developed after the successful generation of a Podocyte Damage Score by PhD student Tsimafei Padvitski. The 'Podocyte Damage Score (PDS) was developed to explore using a gene signature generated in a supervised fashion to measure a relevant phenotype in several disease models. The hypothesis behind the idea of a single cell damage score is that a compact cell-type specific and from disease etiology independent transcriptomic signature of cellular damage exists and it can be used to calculate the damage level of a single cell of said cell-type with disregard of the specific underlying pathology. It is based in the assumption that such a signature can be found using a meta-analysis of a spectrum of gene expression profiles of different disease models affecting the same organ. We learn the compact subset of genes for calculating the HDS on widely available murine bulk RNA-seq data from experiments modeling human liver pathologies. A further reason to use bulk RNA-seq data is that single hepatocytes are difficult to sequence because they

dissociate and can have several nuclei, making single cell RNA-seq data scarce. In the case of the HDS, we call the compact gene signature a 'Universal Hepatocyte Damage Gene Signature' (UHDS). Validation steps are done on mouse single cell and single nucleus RNA sequencing data with a future goal in mind of applying the HDS on single cell or single nuclei human RNA sequencing data for diagnostic or investigative purposes.

These are the steps taken to learn the UHDS for calculating the HDS. First, pre-processing the gene expression counts includes quality control and read alignment of raw counts, as well as exploratory analysis of aligned counts. Next a differential gene expression analysis (DGEA) of each data set is carried out. The output of the DGEA is a set of tables that include the differentially expressed genes ranked in ascending order by their respective p-values. These tables are then merged into a UHDS by including only the genes that fulfill the following criteria:

1) Genes detected in at least 75% of the studies
2) Genes that have the same direction of fold change in at least 75% of the studies (disease versus healthy condition)

An 'average rank' is calculated for each gene that passed the filters. This is done by taking the average rank of that one gene across all DGEA tables. For example: if gene A is ranked in the positions 2, 5, 6 and 2, in four tables then the average rank would be: (2 + 5 + 6 + 2) / 4 = 7.5. Finally, the UHDS is sorted in descending order of the 'average rank'.

With the HDS we pose the hypothesis that UHDS markers should show spatial differences in their distribution *in vivo*. To investigate this hypothesis, we want to know the local abundance of the RNA molecules of two UHDS genes, *Rtn4* and *Slc27a5*, to validate that their expression changes between healthy hepatocytes and hepatocytes with accumulated damage. Therefore, the goal of this experiment was to verify the viability to detect spatial distribution of their gene expression by RNA *in situ* hybridization and produce histological images that can be later analyzed to (semi-)quantify several parameters like RNA abundance and the area of fat droplets. Fat accumulation in hepatocytes should be used as a measure for hepatocyte damage. We focus on the genes *Rtn4* and *Slc27a5* two out of 42 genes included in the most recent version of the UHDS. The former is expected to be upregulated in damaged hepatocytes and the latter to be downregulated such hepatocytes.

The role of these two genes of interest in disease have been previously studied but further analysis is needed to fully understand their involvement in liver pathologies. One of the genes of interest, *Rtn4* encodes for multiple isoforms *Nogo-A, -B* and *-C. Nogo-A* and *-C* are expressed predominantly in the central nervous system, whereas *Nogo-B* is found in many tissues and plays a role in wound healing and vascular remodeling in pathological vascular conditions (Yu et al., 2009)(Acevedo et al., 2004)(Paszkowiak et al., 2007). *Nogo-B* has been described as a regulator of hepatic fibrosis (Zhang et al., 2011).

In the following report, you can find the methods and materials used during the experiments as well as a the results including some exemplary histological microscope images of the murine liver sections after RNA ISH and short discussion section to conclude.

II. Materials

1. Chemicals, Reagents, Kits, and Equipment

Table 1. Chemicals and Reagents

Chemical	Supplier
Xylene (mixture of isomers)	VWR Chemicals
100% EtOH	Werner Hofmann
Meyer's Hematoxylin solution	Sigma-Aldrich
Hematoxylin QS	Vector Laboratories, Inc
Eosin Y solution 0.5 % in water	Meck KGaA
Cytoseal™ XYL Mounting Medium	Thermo Scientific
Vectamount Permanent Mounting Medium	Vector Labs

Table 2. RNAscope® Kits and Reagents

RNAscope® kits and reagents	Supplier
RNAscope® 2.5 HD Duplex Detection Reagents (REF 322500)	Advanced Cell Diagnostics
RNAscope® 2.5 HD Detection Reagent – RED (REF 322360)	Advanced Cell Diagnostics
ImmEdge™ Hydrophobic Barrier Pen	Vector Laboratory
Superfrost Plus™ Gold Adhesion Microscope Slides White Tab	Epredia Netherlands B.V.
RNAscope® Hydrogen Peroxide	Advanced Cell Diagnostics
RNAscope® Protease Plus	Advanced Cell Diagnostics
RNAscope® Target Retrieval Reagents	Advanced Cell Diagnostics
RNAscope® Wash Buffer Reagents	Advanced Cell Diagnostics

Table 3. RNAscope® Probes

RNAscope® Probes	Catalog Number	Supplier
RNAscope® Negative Control Probe-DapB	310043	Advanced Cell Diagnostics
RNAscope® Positive Control Probe Mm-Ppib	313911	Advanced Cell Diagnostics
RNAscope® Probe Mm-Slc27a5 (C1)	508431	Advanced Cell Diagnostics
RNAscope® Probe Mm-Rtn4 (C1)	404661	Advanced Cell Diagnostics
RNAscope® Probe Mm-Alb (C2)	437691	Advanced Cell Diagnostics

Table 4. Equipment

Equipment	Supplier
Leica EG1160 Tissue Embedding Station	Leica Biosystems
Leica RM2255 Fully Automated Rotary Microtome	Leica Biosystems
Drying Oven UN30pa	Memmert
HybEZ™ Humidity Control Tray	Advanced Cell Diagnostics
HybEZ™ Oven	Advanced Cell Diagnostics
ACD EZ-Batch™ Slide Rack	Advanced Cell Diagnostics

Rocker-Shaker PMR-100	Grant-Bio
Stainless-Steel Microtome Balde S35	Feather
Slidescanner Olympus Slideview V5200	Olympus
Heating Table	Medax Gmbh & Co KG

Table 5. Buffer preparation

Buffer	Preparation
20X Saline-Sodium-Citrate (SSC) Buffer	3 M sodium chloride (NaCl) and 300 mM trisodium citrate For 1 L 20175.3 g of NaCl and 88.2 g of trisodium citrate were dissolve in 800 ml distilled water. With a few drops of HCl the pH was adjusted to 7.0 and the volume was adjusted to 1 L with additional distilled water. Solution was sterilized by autoclaving.

2. Mouse Liver Samples

Mouse livers were fixed in as formalin-fixed paraffin-embedded tissue. They stemmed from male mice and were provided by the Wunderlich Group from previous experiments. Animal care, diets and diet experiments used when generating the samples are described in the methods section. The genetic background of the mice was either Stat3-fl (fl/fl) mice with ALFP-Cre (wt/wt) or NIK-fl (fl/fl) mice with ALFP-Cre (wt/wt), considered wildtype in the context of this experiment. Information on animal and care and diet was provided by the group.

2.1. Sample Identifiers and Muse Data per RNAscope® Batch

Batch 0: Alb-Probe

Mouse	DOB	Mutation	Diet	bodyweight (g)	body length (nose to tail, cm)	VAT (g)	liver (g)	tumors < 2mm	tumors <5mm	tumors >5mm
VES-0011455	17.05.2021	Stat3-fl (fl/fl); ALFP-Cre (wt/wt)	NCD	29,80	17,20	0,34	1,43	0	0	0
VES-0011493	14.06.2021	Stat3-fl (fl/fl); ALFP-Cre (wt/wt)	NCD	28,40	17,40	0,48	1,67	0	0	0
VES-0011495	14.06.2021	Stat3-fl (fl/fl); ALFP-Cre (wt/wt)	NCD	28,90	17,30	0,31	1,71	0	0	0
VES-0011166	12.02.2021	Stat3-fl (fl/fl); ALFP-Cre (wt/wt)	CDAA	40,20	NA	1,47	4,57	1	0	0
VES-0011167	12.02.2021	Stat3-fl (fl/fl); ALFP-Cre (wt/wt)	CDAA	39,70	NA	0,88	3,15	5	1	0
VES-0011180	15.02.2021	Stat3-fl (fl/fl); ALFP-Cre (wt/wt)	CDAA	41,80	NA	1,70	2,23	53	8	0

Batch 1: Rtn4-Probe and Slc27a5-Probe

Mouse	DOB	Mutation	diet	bodyweight (g)	body length (nose to tail, cm)	VAT (g)	liver (g)	tumors < 2mm	tumors <5mm	tumors >5mm
VES-0011167	12.02.21	Stat3-fl (fl/fl); ALFP-Cre (wt/wt)	CDAA	39,7		0,88	3,15	5	1	0
VES-0011180	15.02.2021	Stat3-fl (fl/fl); ALFP-Cre (wt/wt)	CDAA	41,80		1,70	2,23	53	8	0
VES-0011493	14.06.2021	Stat3-fl (fl/fl); ALFP-Cre (wt/wt)	NCD	28,40	17,40	0,48	1,67	0	0	0
VES-0011495	14.06.2021	Stat3-fl (fl/fl); ALFP-Cre (wt/wt)	NCD	28,90	17,30	0,31	1,71	0	0	0
VES-0010371		wt/wt	NASH							
VES-0010369		wt/wt	NASH							

Batch 2: Rtn4-Probe and Slc27a5-Probe

Mouse	DOB	Mutation	diet	bodyweight (g)	body length (nose to tail, cm)	VAT (g)	liver (g)	tumors < 2mm	tumors <5mm	tumors >5mm
VES-0011459	17.05.2021	Stat3-fl (fl/fl); ALFP-Cre (wt/wt)	NCD	30,50	17,00	0,24	1,64	0	0	0
VES-0011494	14.06.2021	Stat3-fl (fl/fl); ALFP-Cre (wt/wt)	NCD	27,80	17,50	0,38	1,62	0	0	0
VES-0011192	15.02.2021	Stat3-fl (fl/fl); ALFP-Cre (wt/wt)	CDAA	35,20	16,50	0,87	1,54	44	8	1
VES-0011200	14.02.2021	Stat3-fl (fl/fl); ALFP-Cre (wt/wt)	CDAA	32,24	16,30	1,14	3,27	17	0	0
VES-0010234		wt/wt	NASH							
VES-0010180		wt/wt	NASH							

III. Methods

1. Animal Care, Diets and Sampling of Livers Tissue

All animal tissue samples originated in experiments prior to this project and followed the following methods.

1.1. Animal Care

Animal procedures followed protocols approved by local government authorities (Bezirksregierung Köln) and conducted in accordance with NIH guidelines (84-02.04.2014.A074 and 84-02.04.2014.A074) Permission to maintain and breed mice was issued by the Department for Environment and Consumer Protection - Veterinary Section, Köln, North Rhine-Westphalia, Germany). Mice were kept in individual ventilated cages at 22°C–24°C using a 12-hour light/dark cycle. Animals we given access to water and food *ad libitum* with the only exception being fasting periods required if these were required by the experiment.

1.2. Animal Diets and Feeding experiments

Liver tissue was obtained from mice fed one of three following diets. The nutritional composition of the diets was for the normal chow-diet (NCD) (R/M-H; Ssniff Diet) 57% of calories from carbohydrates, 34% calories from protein and 9% calories from fat, for the EF NASH diet (NASH; E15766-340; Ssniff Diet) the diet contained 42% calories from carbohydrates, 18% of calories from protein and 40 % of calories from fat and for the Choline free, lard,1 % cholesterol diet (CDAA diet; S2159-E042; Ssniff Diet) it contained 58% calories from carbohydrates, 11% of calories from protein and 31% of calories from fat.
For the NASH feeding experiments, male mice were separated from their mothers at p21 into cages with 3-4 littermates. At 6 weeks of age male mice were switched from the NCD diet to respective experimental diets.

1.3. Sampling of murine liver tissue for histology

In general, murine liver tissue samples were cut from the left lateral lobe and the right medial lobe sections placed in a cassette immersed in 10% normal buffered formalin, fixed in 10% NBF for 7 days at room temperature and embedded into paraffin.

2. *In situ* Hybridization with RNAscope® chromogenic Detection Kits

2.1. FFPE Liver Sectioning and Pretreatment for RNAscope® 2.5 chromogenic assay

2.1.1. Sectioning Liver Samples

FFPE mice livers were sliced using a rotary microtome. FFPE containing the livers were placed upside-down on cooling plate at -5 ˚C prior to cutting. The sample holder of the microtome was also cooled. The trimming function was set to 30 µm to remove paraffin sections covering tissue and contamination. Once the sample was properly accessible section thickness was set to 7 µm. Sections were placed in a warm water bath at 42 ˚C directly after cutting. Each section was placed on an adhesion microscope slide and set to dry first on a warm plate and the over-night at 37 ˚C.

For in situ hybridization with albumin three sections were cut per sample, with two sections were being 'back-to-back' (section 1 and 2). In case of the HDS markers the two back-to-back section were cut for each marker per mouse, resulting in fours slices per mouse. Control slides were also considered in each case.

2.1.2. Prepare Materials

Required amount of 1X Wash Buffer by 50X Wash Buffer to autoclaved distilled Milli-Q water and mixed well at RT. Probes were warmed up at 37 ˚C before hybridization and AMP reagents were brought to room temperature before amplification. Humidity Control Tray was wet with autoclaved distilled Milli-Q water and set in HyBEZ Oven to 40˚C.
Target retrieval reagents 630 ml distilled water to 70 ml 10X Target Retrieval Reagents and heated up to 95 ˚C in one liter glass container.

2.1.3. Baking, Deparaffinizing and Pretreatment of FFPE Sections

Slides were baked one hour at 60, then they were incubated in fresh xylene for five minutes at RT, followed by additional five minutes in with fresh xylene at RT with occasional agitation. Sections were then incubated in 100% ethanol for one minute at RT. This step was repeated with fresh 100% ethanol and slides were air dried for five minutes at RT. Next, approx. four drops of RNAscope® Hydrogen Peroxide were applied to cover the entire sections and incubated for ten minutes at RT. After incubation, RNAscope® Hydrogen Peroxide was removed by tapping the slides on absorbent paper and washing them twice by moving them up and down in distilled water three to five times. Target retrieval was performed by cooking the sections in 1 L 1X Target Retrieval Reagents for 30 minutes at 95 ˚C. Then, sections were transferred to a container with distilled water, rinsed for 15 seconds and incubated for three minutes in 100% ethanol at RT. Finally, slides were dried at 60 ˚C.

After drying, with a Inmedge™ hydrophobic pen, a hydrophobic barrier (ca. 2x2 cm) was drawn around tissue and dried a couple of minutes at RT. Next, sections were completely covered with RNAscope® Protease Plus, inserted in the HyBEZ™ humidity control tray and incubated in HyBEZ™ oven for 30 minutes at 40 ˚C. After incubation, protease was removed by tapping slides sideways on absorbent paper and washing with Wash Buffer.

2.2. Hybridization and Amplification

2.2.1. Assay with RNAscope® HD Duplex Detection Kit

Approximately four drops of either *Alb*-Probe, positive control or negative control probes were applied to cover the corresponding sections. Slides were placed inside humidity control tray were incubated in HyBEZ™ oven at 40 ˚C for 2 hours. They were then washed twice with 1X Wash Buffer for 2 minutes at RT with agitation. Slides were kept in 5X SSC overnight at RT.

The following day, slides were washed with 1X Wash Buffer for 2 minutes at RT with agitation. Approx. 4 drops of AMP 1 were applied on each slide. Slides were placed in humidity control tray and incubated in HyBEZ™ oven at 40 ˚C for 30 minutes. Then they were washed twice with 1X Wash Buffer for 2 minutes at RT with agitation.

Approx. 4 drops of AMP 2 were applied on each slide. Slides were placed in humidity control tray and incubated in HyBEZ™ oven at 40 ˚C for 15 minutes followed by two washing steps with 1X Wash Buffer for 2 minutes at RT with agitation. Next, approx. 4 drops of AMP 3 were applied on each slide. Slides were placed in humidity control tray and incubated in HyBEZ™ oven at 40 ˚C for 30 minutes. Then they were washed twice with 1X Wash Buffer for 2 minutes at RT with agitation. Subsequently, approx. 4 drops of AMP 4 were applied on each slide. Slides were placed in humidity control tray, incubated in HyBEZ™ oven at 40 ˚C for 15 minutes and then washed with 1X Wash Buffer for 2 minutes at RT with agitation. Next, approx. 4 drops of AMP 5 were applied on each slide. Slides were placed in humidity control tray, incubated at RT for 30 minutes. Afterwards they were washed twice with 1X Wash Buffer for 2 minutes at RT with agitation. Approx. four drops of AMP 6 were then applied on each slide. Slides were placed in humidity control tray, incubated at RT for 15 minutes and washed twice with 1X Wash Buffer for 2 minutes at RT with agitation. To detect the red signal around 70 µL of a 1:60 Red-B to Red-A working solution mix were applied on every section. Sections were incubated inside the humidity control tray at RT for 10 minutes and then washed twice with 1X Wash Buffer for 2 minutes at RT with agitation. Approx. 4 drops of AMP 7 were applied on each slide. Slides were incubated in the HyBEZ™ oven for 15 minutes at 40 ˚C and washed twice with 1X Wash Buffer for 2 minutes at RT with agitation. Next, approx. 4 drops of AMP 8 were applied on each slide. Slides were placed in humidity control tray and incubated in the HyBEZ™ oven at 40 ˚C for 30 minutes. Afterwards they were washed twice with 1X Wash Buffer for 2 minutes at RT with agitation. All following incubation steps were done at RT. Around 4 drops of AMP 9 solution were applied on slides. Slides were then incubated for 30 minutes and washed twice with 1X Wash Buffer for 2 minutes at RT with agitation. For the final amplification step, around 4 drops of AMP 10 were applied on the slides. Slides were there incubated 15 minutes at RT and then washed twice with 1X Wash Buffer for 2 minutes at RT with agitation. To detect the green signal around 70 µL of a 1:50 Green-B to Green-A working solution mix were applied on every section. Sections were incubated inside the humidity control tray at RT for 10 minutes and washed one last time with 1X Wash Buffer for 5 minutes at RT with agitation. Slides were rinsed quickly with water.

2.2.2. Assay with RNAscope® HD Singleplex Reagent Red

Approximately four drops positive and negative control probes were applied on corresponding section. *Rtn4*-probe was applied on one section of each mouse liver and *Slc27a5*-probe on left over sections. Sections were placed inside humidity tray and incubated in HyBEZ™ oven at 40 ˚C for 2 hours. They were then washed twice with 1X Wash Buffer for 2 minutes at RT with agitation. This is how the washing was performed in all following steps. Slides were kept in 5X SSC overnight at RT.

For Batch 1 there was no overnight pause. For Batch 0 and Batch 2 the slides were kept submerged in 5X SSC overnight at RT and washed twice with 1X Wash Buffer before continuing with the signal amplification steps.

Approximately two to four drops of AMP 1 reagent were added on each section. The slides were then incubated for 30 minutes at 40 ˚C inside the humidity control tray

and in the HyBEZ™ oven. Excess liquid was removed from the slides before washing. Same procedure was repeated with AMP 2 reagent and an incubation time of 15 minutes. After the washing step, AMP 3 reagent was applied, and slides were incubated for 30 minutes at 40 ˚C. Washing was performed after incubation and slides were covered with AMP 4 reagent and incubated for 15 minutes at 40 ˚C . Further amplification steps were performed at RT and the HyBEZ™ oven was turned off. Following a washing step, AMP 5 was applied to cover each section and slides were incubated for 30 minutes. Lastly, after washing, AMP 6 reagent was applied on the sections and incubated for 15 minutes and washed. To detect the signal, approximately 80 µm RED working solution were added to each section. To prepare the RED working solution Fast RED-B and Fast RED-A solutions were mixed in a 1:60 ratio less than 5 minutes before application. Sections were incubated inside the humidity control tray for 10 minutes at RT. Each slide was flicked to remove excess liquid, submerged in tap water, and rinsed again with fresh tap water.

2.3. Counterstaining and Mounting After RNAscope® Assay

Directly after the last washing step, sections were covered with approx. three to two drops of Hematoxylin QS (Vector) and incubated around 30 seconds. For bluing, Slides were then dipped in tap water for 10-15 seconds and washed up and down in fresh tap water 3-4 times. Slides were then dried 30 minutes at 60 ˚C and subsequently cooled down at RT for 5 minutes. Each slide was briefly dipped in xylene to be then immediately covered with 1-2 drops of VectaMount Mounting Medium. A 24 mm by 40 mm coverslip was directly placed over section trying to avoid air bubbles. Slides were airdried overnight.

3. Hematoxylin and Eosin Staining of FFPE liver sections

One of each back-to-back FFPE sections was stained with H&E. Hematoxylin was filtered to avoid clumps before use. Microscope slides containing sections were soaked in xylol for 20 minutes, followed by two minutes in 100% ethanol, two minutes in 96% ethanol, two minutes in 70 % ethanol, one minute in tap water and finally six minutes in hematoxylin. Slides were washed shortly with tap water, and then soaked in tap water for 15 minutes and shortly washed with distillated milli-Q water to be then dipped in eosin for one minute. Slides were then washed six to seven times in tap water, soaked one minute in 70 % ethanol, one minute in 96 % ethanol, one minute in 100 % ethanol and one minute in xylene. Immediately the sections were covered with one or two drops of Cytoseal XYL mounting medium and covered with a 24 by 40 mm microscope cover glass. Slides were left to dry at room temperature.

4. Imaging

Imaging was done using a slide scanner set for bright-field microscopy with x40 magnification and a high to very high concentration of focus points. The images were stored in “vsi” format.

IV. Results

In this section, a selection of representative cropped images of RNAscope® and H&E-staining slide-scans will be showed. There is a total of 40 RNAscope® treated slides and 30 H&E-stained slides. This first section will include the validation of the RNAscope® assay for the mRNA detection of specific genes *in vivo* and *in situ* in mouse liver FFPE sections. First, FFPE mice liver fed either NCD or CDAA diet (N = 3) were assessed by RNAscope® for *in situ* abundance of *Alb* mRNA. Background signal was assayed using moderately expressed house-keeping gene *Ppib* (peptidyl isomerase B) as technical positive control and the bacterial *dapB* gene (dihydrodipicolinate reductase) as negative control. Technical controls show RNA integrity, demonstrating very low DapB background signal and a robust homogenous *Ppib* signal detected in sections from both conditions. A light background staining in the form of green-blue hue could be observed but this could be clearly distinguished from mRNA signals visible as dots. An abundant and homogenous signal of *Alb*-RNA was detected in all liver sections from both conditions (NCD and CDAA, N = 3). *Alb*, which encodes for the protein Albumin, is highly and primarily expressed in the liver. The observed RNA signal is consistent with this (Fig. 1). To avoid confusion, only the initial assessment of the assay (Batch 0) was performed using RNAscope Fast Green Reagent because of its availability. All following RNAscope® experiments were performed with RED reagent. Technical controls (Batch 2) conducted with RED dapB and Ppib probes on NCD and NASH tissue show appropriate RNA integrity and low to no background signal (Figure 2A).

Rnt4 is expected to be expressed in both control and damaged hepatocytes, but up-regulated in the latter. With the RNA *in situ* hybridization, we want to assess the viability to detect *Rtn4* RNA in hepatocytes present in FFPE mouse liver sections. Furthermore, we want to assess if there is an observable difference in gene expression between conditions NCD, NASH and CDAA, and also with regions of the same conditions, i.e., observe if there is a difference in transcript abundance between regions containing more damaged hepatocytes. In Figure 2C we see evenly distributed of Rtn4 expression with some small patches, but expression levels appear to be medium-high around the whole sections. On the other hand, in both CDAA (Fig. 2B) and NASH (Fig. 2D) there seems to be overall higher abundance of transcripts, with many dot clusters. In these conditions, *Rtn4* transcripts are evenly distributed across stretches of hepatocytes with no fat accumulation. *Rtn4* signal increases closer and directly around fat droplets, partly forming dot clusters.

In the case of *Slc27a5* mRNA detection in NCD tissue we see a high number of transcripts evenly distributed across the whole tissue section, with the exception being the cells most proximate to the blood vessels (Fig. 2E). In contrast the Slc27a5 transcript abundance in CDAA tissue looks very uneven. Stretches with high accumulation of fat droplets show a much smaller concentration of transcripts than the areas with less affected hepatocytes (Fig. 2F). These hepatocytes have a high level of *Slc27a5* mRNA, like the distribution seen in NCD tissue. In NASH, the distribution and abundance of Slc27a5-mRNA-signals does not show a clear and homogenous pattern across replicates or even the same tissue section (Fig 3). There is an overall trend of lower *Slc27a5* expression in NASH compared to NCD. Overall, the tissue shows very different abundances of transcripts ‘concentrated’ in big patches with many dot clusters in contrast to the rest of the tissue. Although in one replicate it seems there might a slight concentration of Slc27a5-signal around damaged hepatocytes (Fig. 3C), there are other sections that show no pattern in relation to the fat droplets (Fig. 3B).

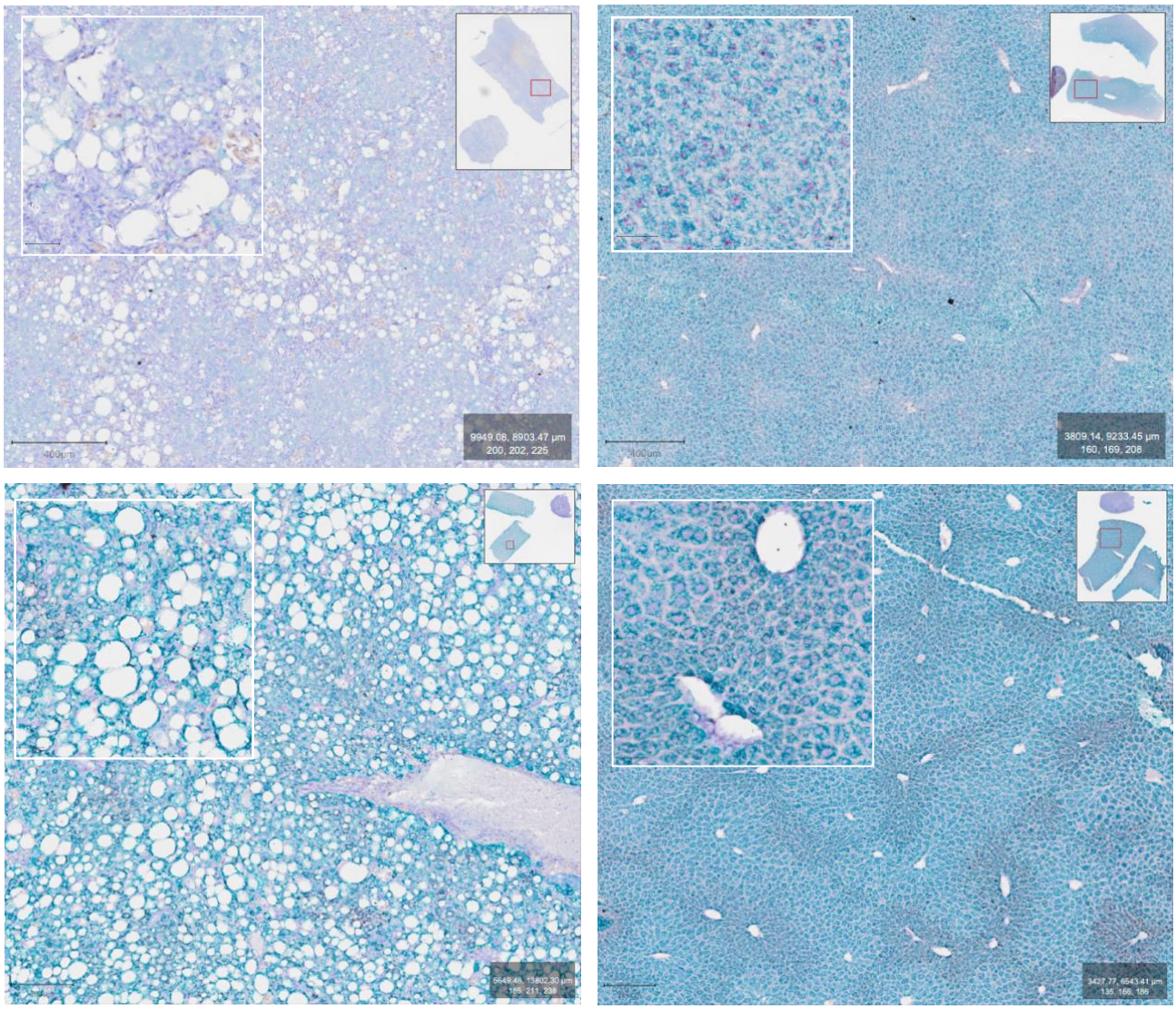

Figure 1. Initial assessment (Batch 0) of RNAscope® of FFPE mouse liver sections of two conditions (N = 3). Green dots are indicate the presence of single RNA molecules detected by the prob. Top left: Technical negative control RNAscope® staining with DabP-Probe of a CDAA liver section (ID: VES0011180). Green 'hue' of tissue can be differentiated from the true signal of detected RNA molecules that are visible as clear dots. Top right: technical positive control RNAscope® staining with Ppi- Probe of NCD liver section (ID: VES0011495). Bottom left: RNAscope® staining of CDAA liver section with Alb-Prob (ID: VES0011166). Bottom right: RNAscope® staining of CDAA liver section with Alb-Prob (VES0011455).

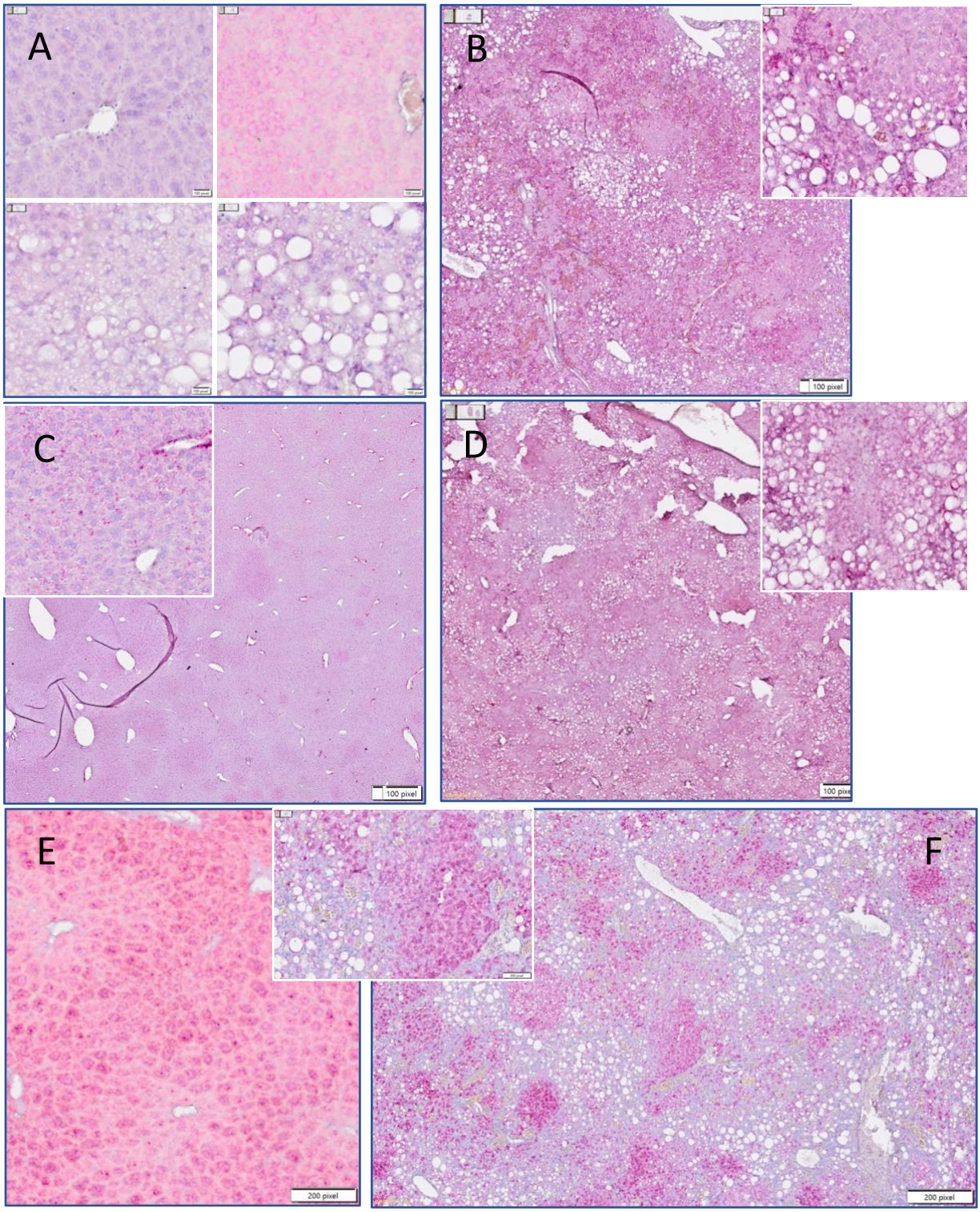

Figure 2. In situ expression of HDS marker genes Rtn4 and Slc27a5 in mouse liver sections in three conditions. *Representative x40 magnification bright-field images of (second batch) RNAscope® RED Reagent assay applied to mouse liver sections of three conditions (NCD, CDAA and NASH, N = 2). Nuclei are stained blue with hematoxylin and red dots indicate the RNAscope® signal from an RNA molecule detected by the corresponding probe. Accumulation of fat in hepatocytes is visible as white circles that resemble "punch holes". Lerger "hole"' with a rather not circular shape are either blood vessels, bile ducts (?) or tears in the tissue. A) Technical controls to check for RNA integrity and well-functioning of assay: Images on the left include sections hybridized with negative control probe (DabP). There is no DabP detected in either the NCD liver section (top-left, ID: VES0011459) nor the NASH section (bottom-left, ID: VES0010180). Right images include section hybridized with positive control probe (Ppib). Ppib-RNA signal detected as expected in both conditions NCD (top-right, ID: VES0011459) and NASH (bottom-right, ID: VES0010180). B, C and D show sections hybridized with probes for HDS marker gene Rtn4. The NCD section in C displays a moderate to high expression of Rtn4 across the whole tissue. Here 100 pixels ~ 500 µm, detail image approx. 10 times bigger. B) CDAA liver section with areas of high fat accumulation (100 pixels ~ 500 µm, detail x4 zoom-in) C) NCD liver section with moderate to high Rtn4-RNA signa across all cells (ID: VES0011459, 100 pixels ~ 100 µm, detail ~ x5, N =2) D) NASH liver section with visible patches of fat-accumulation. In both B and C, higher expression of Rtn4 observable in regions accumulating fat. E and F show sections hybridized with Slc27a5. E) NCD liver section with strong abundance of Slc27a5 RNA across all cells and no fat-accumulation (ID: VES0011459, 200 pixels ~ 100 µm, N = 2). F) CDAA liber section with high fat accumulation. Slc27a5 signal "patches" are observed in regions less to no Slc27a5 expression (ID: CDAA, VES0011192, 200 pixels ~ 500 µm, detail ~ x5, N = 2)*

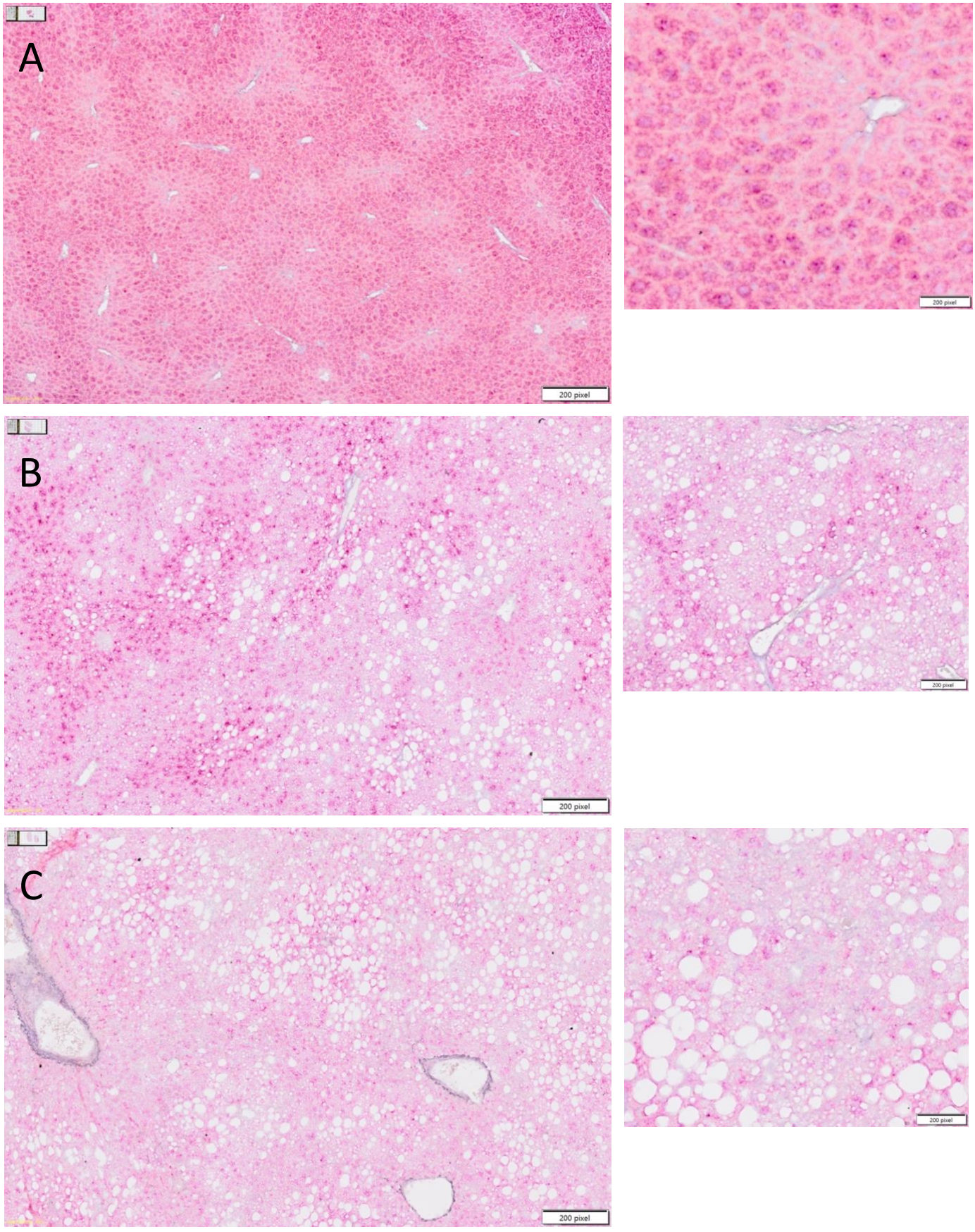

Figure 3. In situ hybridization of Slc27a5 probe in NASH tissue. Representative x40 magnification bright-field images of (second batch) RNAscope® RED Reagent assay applied to NASH mouse liver sections (N = 2). Nuclei are stained blue with hematoxylin and one red dot indicate RNAscope® signal from one hybridized RNA molecule. Accumulation of fat in hepatocytes is visible as white circles that resemble "punch holes". Large, not circular 'punch holes' are mostly blood vessels of different magnitudes. A) NCD liver section with strong abundance of Slc27a5 RNA across all cells and no fat-accumulation (left: VES0011459, 200 pixels ~ 200 µm, right: 200 pixels ~ 50 µm). B) NASH liver section with fat accumulation (left: VES0010180, 200 pixels ~ 200 µm, right: 200 ~ 100 µm). C) NASH liver section with fat accumulation (left: VES0010234, 200 pixels ~ 200 µm, right: 200 pixels ~ 50 µm).

V. Discussion

In a previous project we argued that we can use a 'Hepatocyte Damage Score' to determine the different damage levels of single hepatocytes, given the cells expression of a small subset of genes. This small subset of genes, comprised of 42 ranked genes, should represent a universal damage signature shared across human liver pathologies in the mouse as model system. The goal of this experiment is to investigate two of the genes of the UHDS *in vivo* and we propose the hypothesis that these UHDS markers should show spatial differences in their distribution since the liver tissue is composed of hepatocytes with different levels of damage. For this matter, we assume that areas of the tissue rich in fat droplets can be classified as containing more damaged hepatocytes. Here, we focused on *Rtn4* and *Slc27a5*.

First, we tested the viability of the RNAscope assay on mouse liver tissue fed normal diet (NCD) and CDAA diet using probes to detect *Alb*-RNA and confirmed the viability of this assay. Next, we proceeded with the RNA *in situ* hybridization with probes of the two genes of interest on three conditions (NCD, CDAA and NASH), we observed results matching mostly consistent with our expectations. *Rtn4* transcripts were more abundant in damaged conditions (CDAA) and exhibited a clear zonation, with transcripts accumulating in areas of the tissue rich in fat droplets. This same pattern was observed, but to a lesser degree, in NASH tissue. *Slc27a5* transcript abundance decreased in CDAA and NASH samples. Accordingly in CDAA tissue sections, as proposed by the HDS, transcript accumulation decreased in areas with less fat droplets. However, in NASH samples *Slc27a5* transcripts did not follow any recognizable pattern of zonation. The lack of any recognizable pattern could indicate technical artifact. Therefore, the experiment should be repeated, if possible, with a different set of samples and N = 4.

All observations so far have been estimated by eye. Therefore, to investigate the spatial differences of transcript abundance more accurately, particularly the gene expression spatial differences between areas of the tissue in respect to their degree of damage i.e., fat accumulation, they must be assessed with a quantitative method that allows comparison. An image processing pipeline could be set-up to quantify the number of mRNA molecules (dots) and to measure the area of the fat droplets. For example, QuantISH is an open source program with cell classifier and expression quantification tool that can be used on chromogenic RNA ISH images from various tissues (Jamalzadeh et al., 2022). Nevertheless, we could encounter some challenges since quantifying the number of cells is not trivial in the case of hepatocytes, because most cell recognition algorithms use the nucleus as an orientation point to separate cells, but hepatocytes can often have two nuclei. Additionally, fat droplets (that look like 'punch holes' in the images) can hide 'nuclei' and they can be difficult to tell apart from blood vessels by an automated software. Another potential difficulty is that tissue used in the RNAscope assay cannot be stained with eosin which usually used to in histology to color the cytoplasm. If we successfully achieve to semi-automated signal quantification, we could scale up the experiment for other genes of interest.

Evidence that the HDS markers indeed differentiate locally between cells depending on their level of damage provides further insight on the molecular mechanisms that could be driving or resulting from hepatocellular damage and can ultimately lead to phenotypes we associate with liver disease. By exploring which pathways, the UHDS genes are involved in, and by

having spatial information of their expression, we could better understand the downstream effects shared across different liver disease etiologies. We also speculate, that many genes HDS expects to be downregulated could be part of the loss of tissue identity often associated liver disease (Berasain et al., 2023). Lastly, the differences of the spatial distribution of these transcripts can also contribute to novel insight about the genes' functions.

To conclude, although most results meet our expectations giving experimental validation on the information 'contained' in the HDS we still need a standardized method of RNA-signal quantification.

4 References

Acevedo, L., Yu, J., Erdjument-Bromage, H., Miao, R. Q., Kim, J.-E., Fulton, D., Tempst, P., Strittmatter, S. M., & Sessa, W. C. (2004). A new role for Nogo as a regulator of vascular remodeling. *Nature Medicine*, *10*(4), 382–388. https://doi.org/10.1038/nm1020

Berasain, C., Arechederra, M., Argemí, J., Fernández-Barrena, M. G., & Avila, M. A. (2023). Loss of liver function in chronic liver disease: An identity crisis. *Journal of Hepatology*, *78*(2), 401–414. https://doi.org/10.1016/j.jhep.2022.09.001

Jamalzadeh, S., Häkkinen, A., Andersson, N., Huhtinen, K., Laury, A., Hietanen, S., Hynninen, J., Oikkonen, J., Carpén, O., Virtanen, A., & Hautaniemi, S. (2022). QuantISH: RNA in situ hybridization image analysis framework for quantifying cell type-specific target RNA expression and variability. *Laboratory Investigation*, *102*(7), 753–761. https://doi.org/10.1038/s41374-022-00743-5

Moon, A. M., Singal, A. G., & Tapper, E. B. (2020). Contemporary Epidemiology of Chronic Liver Disease and Cirrhosis. *Clinical Gastroenterology and Hepatology*, *18*(12), 2650–2666. https://doi.org/10.1016/j.cgh.2019.07.060

Paszkowiak, J. J., Maloney, S. P., Kudo, F. A., Muto, A., Teso, D., Rutland, R. C., Westvik, T. S., Pimiento, J. M., Tellides, G., Sessa, W. C., & Dardik, A. (2007). Evidence supporting changes in Nogo-B levels as a marker of neointimal expansion but not adaptive arterial remodeling. *Vascular Pharmacology*, *46*(4), 293–301. https://doi.org/10.1016/j.vph.2006.11.003

Sung, H., Ferlay, J., Siegel, R. L., Laversanne, M., Soerjomataram, I., Jemal, A., & Bray, F. (2021). Global Cancer Statistics 2020: GLOBOCAN Estimates of Incidence and Mortality Worldwide for 36 Cancers in 185 Countries. *CA: A Cancer Journal for Clinicians*, *71*(3), 209–249. https://doi.org/10.3322/caac.21660

Yu, J., Fernández-Hernando, C., Suarez, Y., Schleicher, M., Hao, Z., Wright, P. L., DiLorenzo, A., Kyriakides, T. R., & Sessa, W. C. (2009). Reticulon 4B (Nogo-B) is necessary for macrophage infiltration and tissue repair. *Proceedings of the National Academy of Sciences*, *106*(41), 17511–17516. https://doi.org/10.1073/pnas.0907359106

Zhang, D., Utsumi, T., Huang, H.-C., Gao, L., Sangwung, P., Chung, C., Shibao, K., Okamoto, K., Yamaguchi, K., Groszmann, R. J., Jozsef, L., Hao, Z., Sessa, W. C., & Iwakiri, Y. (2011). Reticulon 4B (Nogo-B) is a novel regulator of hepatic fibrosis. *Hepatology*, *53*(4), 1306–1315. https://doi.org/10.1002/hep.24200